SPECTROSCOPIC AND LUMINESCENCE STUDIES OF Cr^{3+} DOPED CALCIUM SILICATE NANOPHOSPHOR

[1]Sathish. K. N, [2]Chikkahanumantharayappa, [3,*]B. M. Manohara, [4]B.M. Nagabhushana,

[1]Department of Physic, Government First Grade College, Chickballapur-562101, India.

[2]Department of Physics, Vivekananda Degree College, Bengaluru-560055, India.

[3]Department of Physics, Government First Grade College, Davangere-577004, India.

[4]Department of Chemistry, M.S. Ramaiah Institute of Technology, Bengaluru-560054, India,

Abstract : (1-7 mol %) Cr^{3+} doped Calcium silicate nanophosphor was synthesized by a combustion technique. The final product was well characterized by powder X-ray diffraction (PXRD), Field emission scanning electron microscopy (FESEM), Fourier Transform Infra-red spectroscopy (FTIR) and UV Visible optical absorption study of the sample was obtain diffused reflectance spectra (DRS). The PXRD results show that the sample was well crystallized with monoclinic phase. The average crystallite size was estimated using Debye- Scherer's formula, Williamson–Hall (W–H) plots and size-strain plot and was found to be in the range (38 – 52) nm. The energy band gap (Eg) of the samples was estimated using Kubelka- Munk method and found to be in the range from (3.4 – 3.5) eV. Photoluminescence (PL) studies show an intense emission peak at 705 nm when excited at 323 nm, which corresponding to $^2E_g \rightarrow {^4A_{2g}}$ transition of R-line of chromium. It is observed that PL intensity increases with increase in Cr^{3+} concentration and highest PL intensity is observed for 5 mol % doped sample and thereafter it decrease with further increase in Cr^{3+} concentration and this is understood by concentration quenching due to cross relaxation. The Commission International De I-Eclairage (CIE) and Coordinated Color Temperature (CCT) of all the phosphors were well located in red region, which was highly potential phosphor for the fabrication of red component of white light, Also display applications.

IndexTerms - **Combustion technique, Energy Band gap, Photoluminescence, Quenching, CCT,**

1. INTRODUCTION

Transition metal ions doped silicate phosphors have been investigated because of their several advantages over other phosphors. Many experimental results reveal that the $CaSiO_3$ exhibit a favorable matrix for long lasting phosphors when doping different transition metal ions. Further it exhibit ionic and covalent nature due to the presence of Ca^{2+} ions and strong interaction between Si-O, in the SiO_3 group. $CaSiO_3$ has a monoclinic crystal structure with $P2_1/c$ (14) space group and it is one dimensional chains of edge-sharing SiO_4 tetrahedron. In this kind of low-dimensional structure, it was very easy to implant other ions into the host lattice and create traps located at suitable depths that can store the excitation energy and emit light at room temperature. Even though several studies based on rare earth doped $CaSiO_3$ were available [1-4], reports on transition metal ions doped $CaSiO_3$ is very limited in literature using combustion route.

Due to strong visible absorption and emission bands, Cr^{3+} ions show fluorescence in the region 700-1100 nm among widely used transition metal ions in luminescence materials. The unfilled $3d^3$ electronics shell of the Cr^{3+} ion has a number of low-lying energy levels, among which optical transitions occur, generating luminescent emission. The optical properties of the Cr^{3+} ions were directly affected by the static and dynamic properties of their environment and the associated optical spectra was characterized by both sharp and broad emission bands since 3d electrons was outside of the ion core [5-8].

In the development of long lasting persistent luminescence materials treated with Cr^{3+}, $CaSiO_3$ as an excellent host because Cr^{3+} ions can easily substitute Cr^{3+} ions and the suitable host lattices crystal field strength around Cr^{3+} ions. For red photoluminescence, trivalent chromium ion (Cr^{3+}) was a favorable emitting center due to its wide-range emission from 700 to 1400 nm, including the R-line narrowband emission around 700 nm from the $^2E_g \rightarrow {^4A_{2g}}$ transition and the broadband 705 nm emission from the $^4T_{2g} \rightarrow {^4A_{2g}}$ transition depending on the host lattices crystal field strength [9-13].

In this paper, $CaSiO_3$:Cr^{3+} (1-7 mol %) phosphor has been synthesized by self-propagating combustion synthesis (CS) method. The CS process was safe, instantaneous and capable of producing single phase compounds at nano level. To the best of our knowledge, there are no reports available on the synthesis and photoluminescence study of $CaSiO_3$:Cr^{3+} (1-7 mol %) via CS process with Citric acid as a fuel. The nature and structural details of the synthesized phosphor was investigated by powder X-ray diffraction (PXRD), Field emission scanning electron microscopy (FESEM), Fourier transform infrared spectroscopy (FT-IR) techniques. The optical properties of $CaSiO_3$:Cr^{3+} phosphor was investigated by UV-Visible absorption and photoluminescent (PL) studies.

2   EXPERIMENTAL

2.1   Synthesis of Cr³⁺ doped cadmium silicate nanophosphor.

(1-7 mol %) Cr^{3+} doped Calcium silicate nanophosphors were synthesized by combustion method by using Citric acid as a fuel [14]. The stoichiometric composition of the redox mixture was calculated by taking the ratio of total oxidizing valencies (O) to the reducing valencies (F) equal to unity i.e., (O/F=1) so that maximum energy was released during combustion. The flow chart for the preparation of $CaSiO_3:Cr^{3+}$ (1-7 mol %) was shown in Fig.1. Analar grade Calcium nitrate (Ca $(NO_3)_2 \cdot 4H_2O$; Sigma Aldrich, 99.9 %), fumed silica (SiO_2, 99.9 %), Chromium nitrate (Cr $(NO_3)_3$, 99.9 %) and Citric acid ($C_6H_8O_7$) were used as the starting materials. An appropriate amount of $Ca(NO_3)_2 \cdot 4H_2O$, SiO_2 and $C_6H_8O_7$ (1:1:1.25 in mole ratio) were well dissolved in ~50 ml of double distilled water and stirred well using magnetic stirrer to get homogenized aqueous solution. The mixture was rapidly heated in a muffle furnace maintained at 500 ± 10 °C. The reaction takes place within few seconds by heating the redox mixture to incandescence leading to the formation of powder. The obtained final product was further calcined at 900 °C for 3 h for the formation of well crystalline sample.
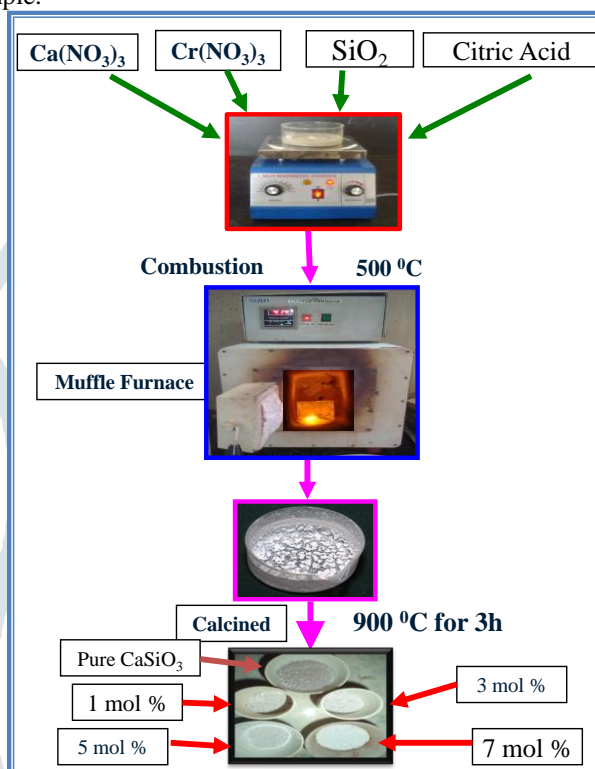

Fig.1. Flow chart of preparation of (1-7 mol%) Cr^{3+} doped $CaSiO_3$ nanophosphor calcined at 900 °C for 3 h.

2.2 CHARACTERIZATION

Powder X-ray diffraction (PXRD) analysis was performed using X'PERT pro Philips analytical diffractometer (operating at 50 KV and 20 mA by means of CuK_α (1.541Å) radiation with a nickel filter at a scan rate of 2° min⁻¹). The data was collected in the range 20^0 to 60^0. Morphology of the sample was analyzed by using a field emission scanning electron microscope (FESEM) (ULTRA55, FESEM (Carl Zeiss) with EDS). Fourier transform infrared (FTIR) spectra was recorded in absorption mode with Perkin Elmer spectrometer (Spectrum 1000) along with KBr pellets. The UV Visible optical absorption study of the sample was made in the range (200–800) nm using Perkin Elmer Lambda 19 to obtain diffused reflectance spectra (DRS). Photoluminescence (PL) studies are made using using Agilent technologies, model Cary Eclipse, Spectroflourimeter at room temperature (RT).

3. RESULTS AND DISCUSSION

3.1 Powder X-Ray Diffraction (PXRD)

Fig. 2 shows the PXRD patterns of (1-7 mol %) of Cr^{3+} doped Calcium silicate calcined at 900 °C for 3 h. The diffraction peaks of Cr^{3+} doped Calcium silicate was well matched with the JCPDS card No. 84-0655 [15] and shows better crystallinity and single monoclinic phase. The average crystallite size was estimated by employing the Debye- Scherrer's formula [16, 17].

$$d = \frac{k \lambda}{\beta \cos\theta} - - - - -(1)$$

where 'β'; the full width at half maximum (FWHM) of the prominent diffraction peaks, 'λ'; the wavelength of X-ray (λ=1.5405Å) used, 'θ'; the Bragg's angle and 'k'; the Scherrer's constant. The average crystallite size of the Cr^{3+} doped Calcium silicate calcined at 900 °C for 3 h was in the range 32-52 nm.
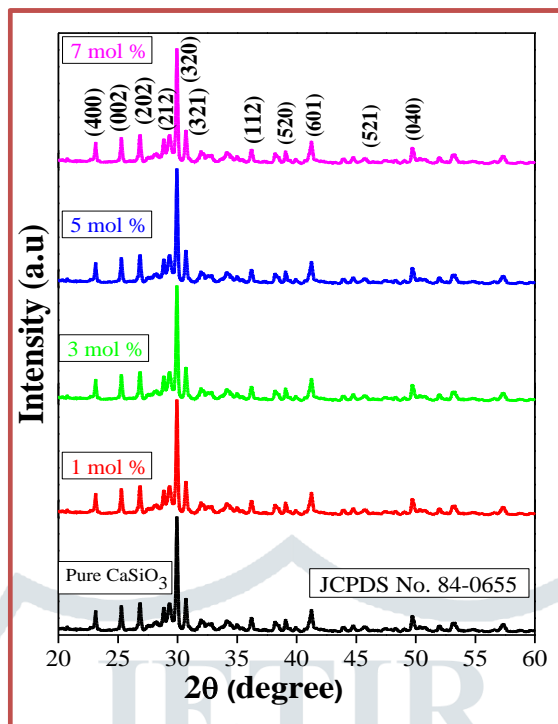
Fig.2. PXRD patterns of undoped and (1-7 mol%) Cr^{3+} doped $CaSiO_3$ nanophosphor calcined at 900 ºC for 3 h.

Lattice strain present in the (1-7 mol %) Cr^{3+} doped Calcium silicate calcined at 900 ºC for 3 h nanophosphor prepared was estimated using the Williamson–Hall (W–H) plots. It was known that the FWHM can be expressed as a linear combination of the contribution from the lattice strain and crystalline size [18].

$$\beta \cos\theta = \frac{k\lambda}{D} + 4\varepsilon \sin\theta ----- (2)$$

Where, 'β'; the FWHM (in radians), 'θ' is the Bragg angle of the peak, 'λ'; the wavelength of X-ray used, 'D'; the effective particle size and 'ε'; the effective lattice strain [19]. The effective particle size for which the lattice strain has been taken into account can be estimated from the extrapolation of the plot as shown in Fig.3. From the W-H plots the lattice strain is extracted from the slope and the crystalline size is extracted from the y-intercept of the linear fit. The average crystallite size estimated from these methods were shown in the Table 1.
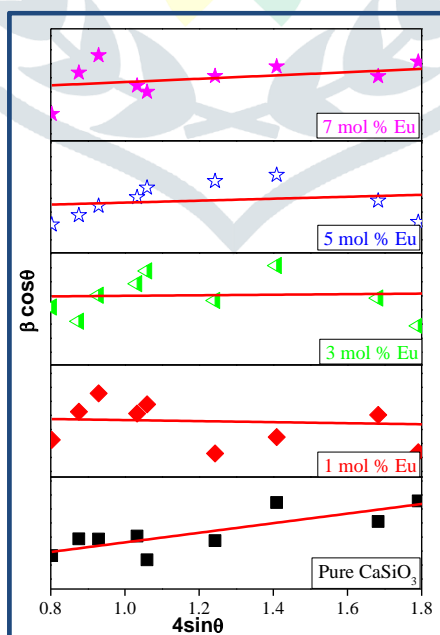

Fig.3. W-H plots of undoped and (1-7 mol%) Cr^{3+} doped $CaSiO_3$ nanophosphor the lattice strain is extracted from the slope and the crystalline size is extracted from the y-intercept of the fit.

3.2 MORPHOLOGICAL ANALYSIS

Field effect electron scanning microscopes (FESEM) were important tool for the characterization of nano materials, as they give information about the morphology of the materials. FESEM and energy dispersive X-ray analysis (EDAX) of CaSiO₃: Cr³⁺ (1-7 mol %) nanophosphor calcined at 900 °C for 3 h was shown in Fig.5(a-e). It was observed that the sample was highly porous, agglomerated, voids and flufy with polycrystalline nature. The pores and voids can be attributed to the large amount of gases escaping out of the reaction mixture during combustion.
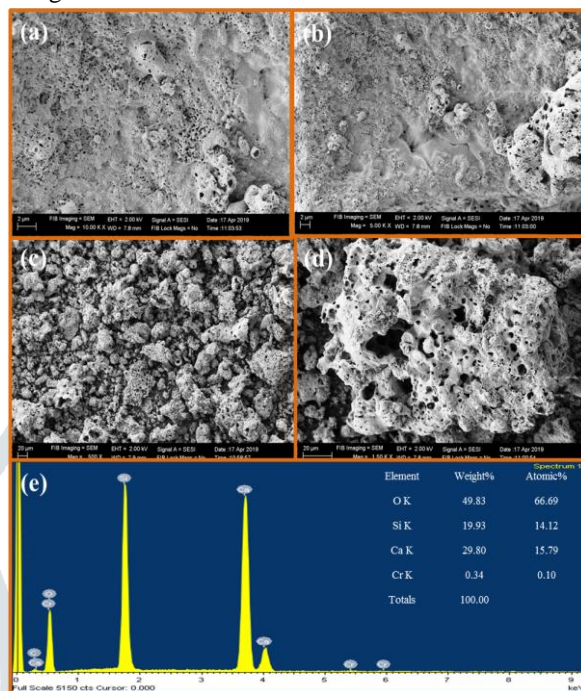

Fig.4. FESEM micrographs of (a) 1 mol% (b) 3 mol% (c) 5 mol% (d) 7 mol% and (f) EDAX (5 mol%) and inset table shows elemenst with atomic weight % of Cr^{3+} doped $CaSiO_3$ nanophosphor.

Table-1: Estimated structural parameter values in undoped and (1-7 mol%) Cr^{3+} doped $CaSiO_3$ nanophosphor

Sl. No.	mol %	Scherer's equation. in nm.	W-H Plot. in nm.	Lattice strain $\epsilon \times 10^{-3}$
01	Pure	38	40	0.24
02	1	49	52	0.62
03	3	48	50	0.35
04	5	39	42	0.17
05	7	40	46	0.46

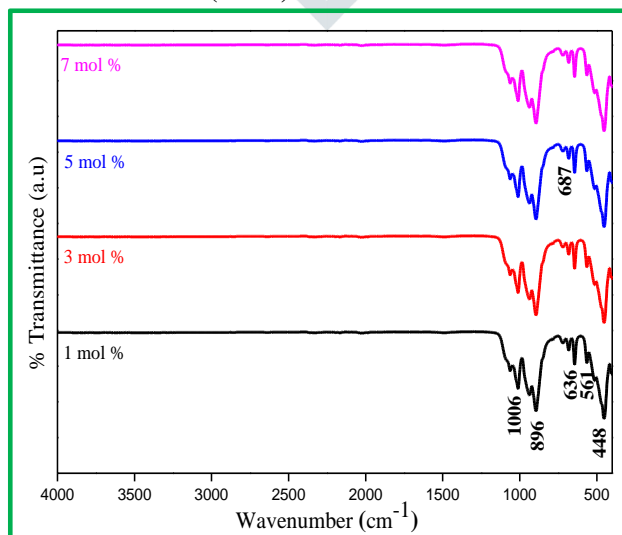## 3.3 FOURIER TRANSFORMATION INFRARED (FTIR) SPECTROSCOPY

Fig.5. FTIR of (1-7 mol %) Cr^{3+} doped $CaSiO_3$ nanophosphor.

In order to investigate the nature of the chemical bonds formed in the prepared sample, FTIR spectra was recorded in the range $4000\text{-}400$ cm^{-1} (Fig.4). The spectra shows the broad band in the range $896\text{–}1006$ cm^{-1} was due to asymmetric stretching vibration of Si–O–Si bond and stretching vibrations of terminal Si–O bonds. The peaks at 448 and 561 cm^{-1} were the characteristic stretching vibrations of Si–O–Si bridges. The sharp peak corresponding to 636 and 687 cm^{-1} can be ascribed to Si–O bond, which exists in the form of SiO_3 [20, 21].

3.4 UV-Visible absorption

The UV–Vis absorption spectra of $CaSiO_3$**:** Cr^{3+} (1-7 mol %) nanophosphor calcined at 900 ^0C for 3 h samples were shown in inset Fig. 6. It was well established that nanoscale materials have large surface to volume ratio. This results in the formation of voids on the surface as well inside the agglomerated nanoparticles. Such voids can cause fundamental absorption bands in the UV region. In addition, surface of nanoparticles were well known to comprise of several defects normally dangling bonds, regions of disorder and absorption of impurity species that result in the absorption of nanocrystals. The optical energy gap (E_g) of $CaSiO_3$**:** Cr^{3+} (1-7 mol %) nanophosphor calcined at 900 ^0C for 3 h. The energy gap (E_g) was evaluated by Kubelka- Munk method, DRS of the material was converted to the absorption spectra by using Kubelka – Munk function [36] and the value of the band gap as shown in Fig.7. The estimated value of E_g was found to be in the range of $(3.4 – 3.5)$ eV. It was observed from the spectra the Eg values were shifting with increase of Cr^{3+} concentrations, which was attributed to quantum confinement effect [22].
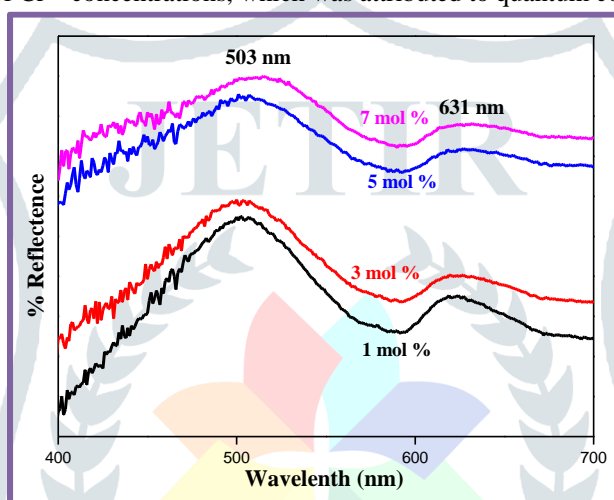

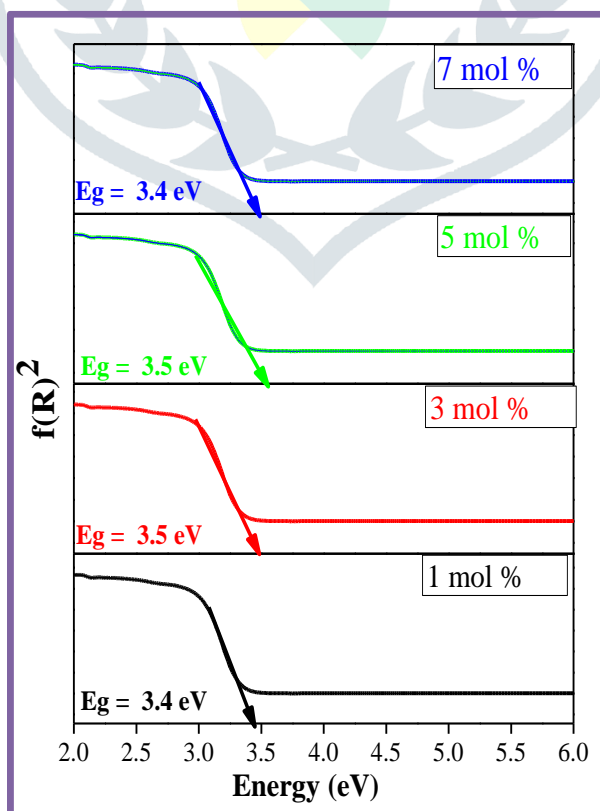Fig.6. UV Visible absorption spectra of (1-7 mol %) Cr^{3+} doped $CaSiO_3$ nanophosphor

Fig.7. Energy band gap of FTIR of (1-7 mol %) Cr^{3+} doped $CaSiO_3$ nanophosphor

3.5 PHOTOLUMINESCENCE (PL) STUDIES

Optical spectroscopy of Cr^{3+} in solids provides important information for understanding the fundamental interactions between the luminescent ion and the lattice. The emission spectra of (1-7 mol %) Cr^{3+} doped $CaSiO_3$ nanophosphor measured at 323 nm excitation was shown in the Fig. 8. The emission bands at 562, 697, 705, 710, 718 and 726 nm observed were attributed to Cr^{3+} ions [23-25]. The strongest emission peak at 707 nm corresponding to $^2E_g \rightarrow {}^4A_{2g}$ was due to hypersensitive forced electric-dipole transition. For low crystal field materials, the quartet ($^4T_{2g}$) was lower and the luminescence emission at 300 K of the system is dominated by spin allowed broad band transition. This is due to the fact that the valence electron in the $3d^3$ configuration was not shielded from their environment by the core electrons. Thus the crystal field, or the lattice environment, has a significant effect on the quantum states of these electrons. Further, the configurationally coordinate model was successful in explaining the shape of the broadband transition. [26]. The variation of PL intensity with different Cr^{3+} concentration was studied and shown in Fig. 9. It was evident from the figure that PL intensity increases with increase in Cr^{3+} concentration up to 5 mol% and thereafter it decrease with further increase in Cr^{3+} concentration and this is understood by concentration quenching due to cross relaxation. As dopant concentration of Cr^{3+} increases, $^2E_g \rightarrow {}^4A_{2g}$ transition dominates and the emission intensity increases. This may be attributed to the increase in distortion of the local field around the Cr^{3+} ions. Moreover, there was charge imbalance in the host lattice due to doping of trivalent Cr^{3+} cations. It was shown that relative intensity of the emission lines of Cr^{3+} depends on the doping concentration of Cr^{3+} in $CaSiO_3$ nanophosphor. As Cr^{3+} concentration increases the transition centered at $^2E_g \rightarrow {}^4A_{2g}$ (705 nm) shows an enhanced emission up to 5 mol % of Cr^{3+}. Further, increase in Cr^{3+} concentration more than 5 mol % the PL intensity decrease due to concentration quenching. When the dopant concentration increases the distance between Cr^{3+} cations decreases, leading to an effective energy transfer between the neighboring cations. Hence, the excited atom moves to the quenching sites, dissipating the energy non-radiatively. As a result of the concentration quenching the emission intensity decreases.
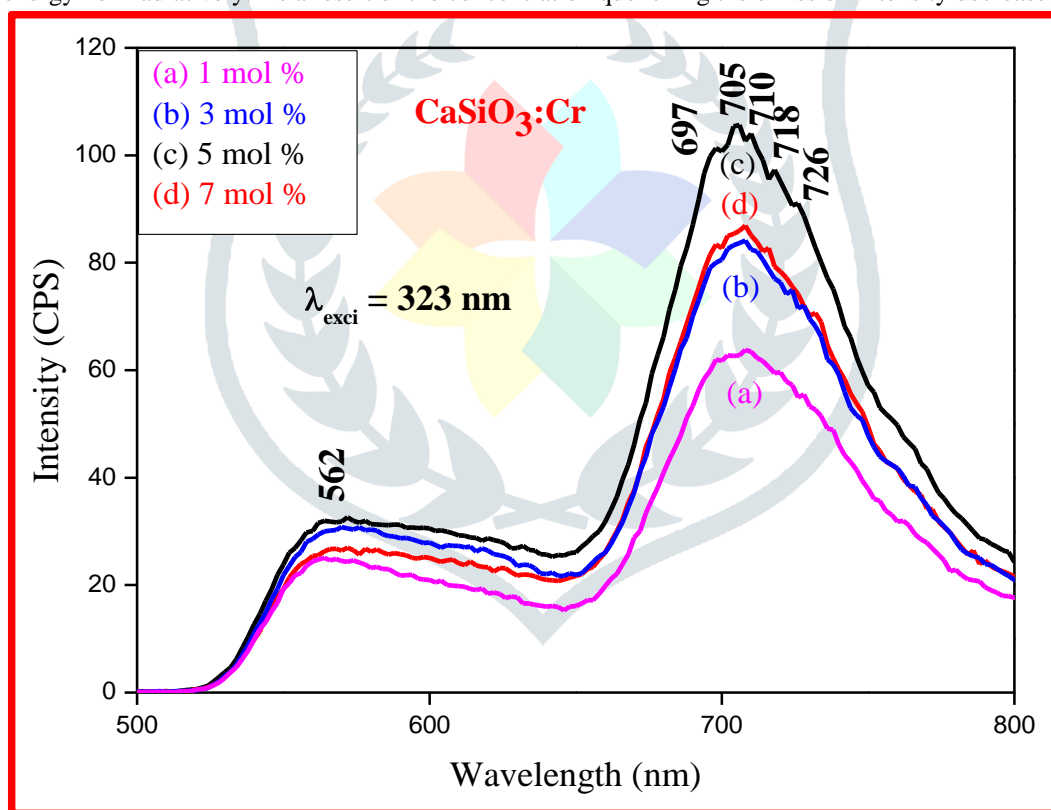
Fig.8. PL Emission spectra of (1-7 mol%) Cr^{3+} doped $CaSiO_3$ nanophosphor excited at 323 nm

The critical energy transfer distance (R_c) was calculated by the following equation:

$$R_c \approx 2\left[\frac{3V}{4\pi X_c N}\right]^{1/3} - - - - -(3)$$

where X_c; the critical concentration, N; the number of cation sites in the unit cell, and V; the volume of the unit cell. For $CaSiO_3$: Cr^{3+} nanophosphor the values of N, V and X_c were 6, 409.85 $Å^3$ and 0.05 respectively. Using these parameters, the estimated Rc is found to be 13.78 Å. Since R_c was not less than 5Å, exchange interaction was not responsible for non radiative energy transfer process from one Cr^{3+} ion to another Cr^{3+} ion in this host.

According to Blasse theory [27], non radiative energy transfer between different Cr^{3+} ions in $CaSiO_3$ phosphor may occur by radiative exchange multipole-multipole interaction. Usually, radiative re-absorption mechanism comes into effect only when there was broad overlap of emission peaks of the sensitizer and activator. In the present case, radiative - reabsorption was completely ruled out as there were no broad overlapping peaks. Therefore, multipolar interaction was used to explain the concentration quenching mechanism. Multipolar interaction involves several types of interaction such as dipole-dipole (d-d), dipole-quadropole (d-q), quadropole-quadropole (q-q) interaction. As a result, the energy transfer process of Cr^{3+} in $CaSiO_3$ phosphor would be due to multipolar interaction.
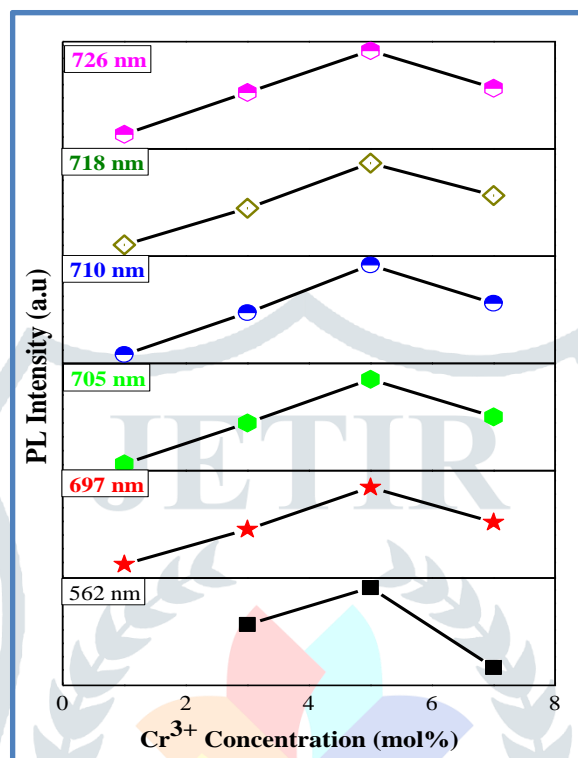

Fig.9. The variation of PL intensity with different Cr^{3+} concentration.

In order to decide the type of interaction involved in the energy transfer Van Uitert's [28] proposed an equation:

$$\frac{I}{X} = k\left[1 + \beta(X)^{Q/3}\right]^{-1} ----- (4)$$

where I; the integral intensity of emission spectra from 550-750 nm, X; the activator concentration, I/X; the emission intensity per activator (X), β and K; constants for a given host under same excitation condition. According to above equation, Q = 3 for the energy transfer among the nearest neighbor ions, while Q = 6, 8 and 10 for d-d, d-q and q-q interactions respectively. Assuming that $\beta(X)^{Q/3} \gg 1$, above equation can be written as

$$\log\left(\frac{I}{X}\right) = K' - \frac{Q}{3}\log X \, (K' = \log K - \log \beta) ----- (5)$$

From equation (5), the multipolar character (Q) can be obtained by plot log (I/X) vs log (X) as shown in Fig.13. The slope and multipolar character 'Q' was found to be - 2.11261 and 4.7937 which was close to 6. Therefore, the concentration quenching in $CaSiO_3$: Cr^{3+} phosphor occurred due to dipole to dipole interaction.

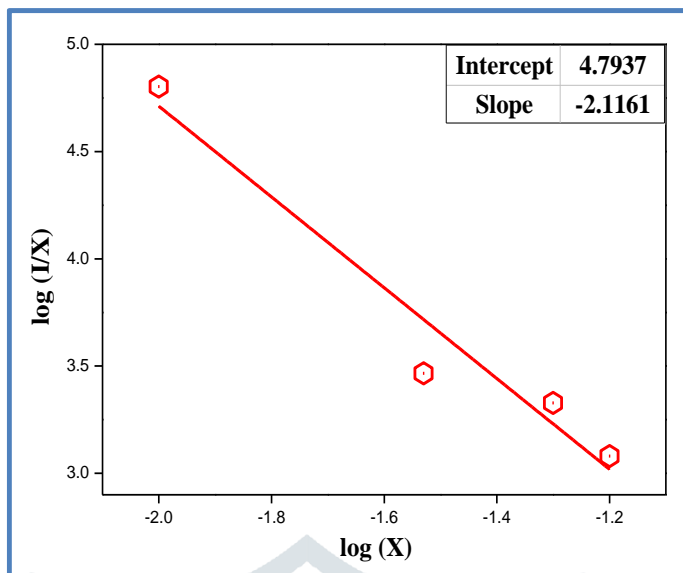| Intercept	4.7937
Slope	-2.1161

Fig.10. Relation between log (x) vs log (I/x) in CaSiO$_3$:Cr^{3+} nanophosphor.

The Commission International De I-Eclairage (CIE) 1931 chromaticity coordinates for CaSiO$_3$: Cr^{3+} (1-7 mol%) phosphors as a function of Cr^{3+} concentration for the luminous color was depicted by the PL spectra. CaSiO$_3$: Cr^{3+} clearly exhibited the excellent CIE coordinates. According to our knowledge, the CIE coordinates of red emission of Cr^{3+} ions not only depend upon the asymmetric ratio but also depend upon the higher energy emission levels. Literature reveal that the Cr^{3+} doping effect become stronger in the case of particles with higher crystallinity, resulting in an improved activation degree of Cr^{3+} (hence the improved red color emission). Their corresponding locations were marked in Fig.11 (a) with stars in red region, their X and Y values were given in the table inset of Fig. 11(a).

The Coordinated Color Temperature (CCT) values were well located in the red region shown in the star mark Fig. 11(b). CCT can be estimated by Planckian locus. This defines the color temperature of a light source. Calculated values of CCT shown inset table of Fig 11(b) by using transforming equations 6 and 7 shows the temperature of the closest point of the Planckian locus to the light source on the (U′, V′) uniform chromaticity diagram 11(b).

$$U' = \frac{4x}{-2x+12y+3} \text{-----------------------} (6)$$

$$V' = \frac{9y}{-2x+12y+3} \text{-----------------------} (7)$$

The average CCT value of prepared Cr^{3+} doped Calcium silicate nanophosphor is 3811 K which was very close to the NTSC standard values [29]. This shows that strongest emission peak shows at 5 mol % Cr^3 doped calcium silicate nanophosphor were potential materials for the fabrication of red component of WLEDs and solid state display applications.
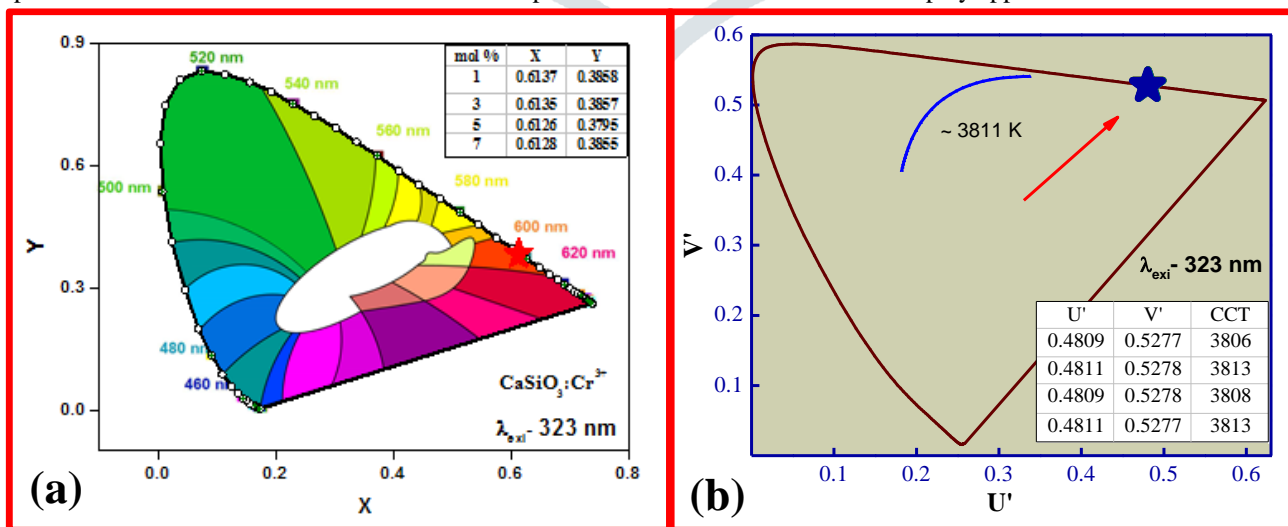

Fig.11(a). CIE chromaticity diagram and (b) CCT of (1-7 mol%) Cr^{3+} doped CaSiO$_3$ nanophosphor.

4. CONCLUSION

Red CaSiO$_3$:Cr^{3+} (1-7 mol %) phosphor was successfully prepared via combustion technique. The average crystallite size was estimated from Debye- Scherer's formula and W-H plots. Photoluminescence emission spectra show that there is increase in emission intensity with increase in Cr^{3+} concentration and beyond 5 mol% concentration quenching is observed. The narrow red emission peak, observed at 705 nm in CaSiO$_3$:Cr^{3+} is due to $^2E_g \rightarrow {}^4A_{2g}$ transition from Cr^{3+} ions. The CIE chromaticity co-ordinates and CCT situated in the red region, hence the phosphor might be useful in red component of WLEDs and display applications.

REFERENCES

[1] M.F. Tsai, S.H.G. Chang, F.Y. Cheng, V. Shanmugam, Y.S. Cheng, C.H. Su, C.S. Yeh, ACS Nano 7 (2013) 5330–5342.

[2] L.C.V. Rodrigues, H. F. Brito, J. Holsa, R. Stefani, M. C.F.C. Felinto, M. Lastusaari, T. Laamanen, L.A.O. Nunes, J. Phys. Chem. C, 116 (2012) 11232−11240.

[3] R. Krsmanovic, Z. Antic, I. Zekovic, M. D. Dramicanin, J. Alloys Compds, 480 (2009) 494–498.

[4].M. O. Onani and F. B. Dejene, "Photo-luminescent properties of a green or red emitting Tb^{3+} or Eu^{3+} doped calcium magnesium silicate phosphors," Phys. B Phys. Condens. Matter, vol. 439, pp. 137–140, 2014.

[5] Yu Teng a, Jiajia Zhou a, Said Nasir Khisro a, Shifeng Zhou a, Jianrong Qiu, Persistent luminescence of SrAl$_2$O$_4$: Eu^{2+}, Dy^{3+}, Cr^{3+} phosphors in the tissue transparency window, Materials Chemistry and Physics 147 (2014) 772-776.

[6] H.N. Bordallo, R.W. Henning, L.P. Sosman, R.J.M. da Fonseca, A. Dias Tavares Jr.,K.M. Hanif, G.F. Strouse, J. Chem. Phys. 115 (2001) 4300-4305.

[7] H.N. Bordallo, X. Wang, K.M. Hanif, G.F. Strouse, R.J.M. da Fonseca, L.P. Sosman,A. Dias Tavares Jr., J. Phys. Condens Matter 14 (2002) 12383-12389.

[8] Vijay Singh, R.P.S. Chakradhar, J.L. Rao, S.H. Kim, EPR and luminescence studies of Cr^{3+} doped MgSrAl$_{10}$O$_{17}$ phosphor synthesized by a low-temperature solution combustion route, Journal of Luminescence 154 (2014) 328–333.

[9] Yinhai Wang , Ke Xu, Darong Li, Hui Zhao, Zhengfa Hu.Persistent luminescence and photocatalytic properties of Ga$_2$O$_3$:Cr^{3+}, Zn^{2+} phosphors, Optical Materials 36 (2014) 1798–1801.

[10] Y.Y. Lu, F. Liu, Z. Gu, Z. Pan, J. Lumin. 131 (2011) 2784–2787.

[11] T.Y. Tomm, P. Reiche, D. Klimm, T. Fukuda, J. Cryst. Growth 220 (2000) 510–514.

[12] T.H. Yeom, I.G. Kim, S.H. Lee, S.H. Choh, Y.M. Yu, J. Appl. Phys. 93 (2003) 3315–3319.

[13] Y. Hou, J. Zhang, Z. Ding, L. Wu, Powder Technol. 203 (2010) 440–446.

[14] K.C. Patil, M.S. Hegde, Tanu Rattan, S.T. Aruna, Chemistry of Nanocrystalline Oxide Materials, Combustion Synthesis, Properties and Applications, World Scientific Publishing Co. Pvt. Ltd., Singapore, 2008.

[15] Lei Zhou, Bing Yan, Sol–gel synthesis and photoluminescence of CaSiO$_3$:Eu^{3+} nanophosphors using novel silicate sources, Journal of Physics and Chemistry of Solids, 69-11 (2008) 2877-2882..

[16] X. Qu, L. Cao, W. Liu, G. Su, H. Qu, C. Xu, P. Wang, J. Alloys Compd. 494 (2010) 196-198.

[17] Y.L. Liu, J.Y. Kuang, B.F. Lei, C.S. Shi, J. Mater. Chem. 15 (2005) 4025-4031.

[18] P. Klug, L.E. Alexander, In: X-ray Diffraction Procedure, Wiley, New York, 1954.

[19] G.K. Williamson, W.H. Hall, Acta Metall. 1 (1953) 22-31.

[20 D.V. Sunitha, H. Nagabhushana, S.C. Sharma, Fouran Singh, B.M. Nagabhushana, N. Dhananjaya, C. Shivakumara, R.P.S. Chakradhar, J. Lumin. 143 (2013) 409-417.

[21] N. Dhananjaya, H. Nagabhushanan, B.M. Nagabhushana, B. Rudraswamy, C. Shivakumara, K.P. Ramesh, R.P.S. Chakradhar, Physica B. 406 (2011) 1639-1644.

[22] A. Escobedo Morales, E. Sanchez Mora, U. Pal, Use of diffuse reflectance spectroscopy for optical characterization of un-supported nanostructures, Rev. Mexic. De Fisica S 53 (2007)   18-22.

[23]. Michael Gaft, Renata Reisfeld, Gerard Panczer, Modern Luminescence Spectroscopy of Minerals and Materials, Springer, 2005, p. 170.

[24]. Carolina M. Abreu, Ronaldo S. Silva, Mário E.G. Valerio, Zélia S. Macedo, J. Solid State Chem. 200 (2013) 54–59.

[25]. V. Singh, R. P. S. Chakradhar, J. L. Rao, and H.-Y. Kwak, "EPR and photoluminescence properties of combustion-synthesized ZnAl$_2$O$_4$:Cr^{3+} phosphors," J. Mater. Sci., vol. 46, no. 7, pp. 2331–2337, Nov. 2010.

[26]   B. S. Ravikumar, H. Nagabhushana, S. C. Sharma, Y. S. Vidya, and K. S. Anantharaju, "Calotropis procera mediated combustion synthesis of ZnAl$_2$O$_4$:Cr^{3+} nanophosphors: Structural and luminescence studies," Spectrochim. Acta Part A Mol. Biomol. Spectrosc., Oct. 2014.

[27]. G. Blasse, Philips Res. Rep. 24 (1969) 131-144.

[28]. L.G Van Uitert. J. Electrochem. Soc. 114 (1967)1048-1053.

[29]. B. M. Manohara, H. Nagabhushana, K. Thyagarajan, B. D. Prasad, S.C. Prashantha, S. C. Sharma and B. M. Nagabhushana, "Spectroscopic and luminescence studiesof Cr^{3+} doped cadmium silicate nano-phosphor," J. Lumin., 161 (2015) 247–256.